



PREDICTION OF INPUT ENERGY SPECTRUM: ATTENUATION MODELS AND VELOCITY SPECTRUM SCALING

F.S. Alici⁽¹⁾, H. Sucuoğlu⁽²⁾

⁽¹⁾ Research Assistant, Department of Civil Engineering, Middle East Technical University, Ankara, Turkey, fsalici@metu.edu.tr

⁽²⁾ Professor, Department of Civil Engineering, Middle East Technical University, Ankara, Turkey, sucuoglu@metu.edu.tr

Abstract

Energy based approaches have a significant advantage in performance assessment since excitation and response durations, accordingly energy absorption and dissipation characteristics are directly considered. Energy based procedures mainly consist of the prediction of earthquake input energy imposed on a structural system during an earthquake, and energy dissipation performance of the structure.

The presented study focusses on the prediction of earthquake input energy. A large number of strong-ground motions have been collected from the NGA database, and parametric studies have been conducted for considering the effects of soil type, epicentral distance, moment magnitude and the fault type on input energy. Then prediction equations for input energy spectra, which are expressed in terms of the equivalent velocity (V_{eq}) spectra, are derived in terms of these parameters. Moreover, a scaling operation has been developed based on consistent relations between pseudo velocity (PS_V) and input energy spectra. When acceleration and accordingly velocity spectrum is available for a site from probabilistic seismic hazard analysis, it is possible to estimate the input energy spectrum by applying velocity scaling. Both of these approaches are found successful in predicting the V_{eq} spectrum at a site, either from attenuation relations for the considered earthquake source, or from the results of probabilistic seismic hazard analysis conducted for the site.

Keywords: input energy, energy demand, energy equivalent velocity, attenuation relations, velocity spectrum scaling

1. Introduction

Performance or displacement based design procedures offer a more realistic approach in earthquake resistant design, compared to capacity design principles, where maximum member deformations are employed as the basic structural response parameters in evaluating structural performance. However, the level of damage on structural components during seismic response do not only depend on maximum deformations, but also on the response history characteristics. A structural component accumulates more damage as its energy dissipation capacity is exhausted whereas this capacity is not independent of the excitation as assumed in force and displacement based design, but strongly depends on the loading history [1, 2]. Therefore, this is a complicated nonlinear problem.

Energy based procedures may offer more comprehensive solutions, and if the energy loaded on a structure under a design earthquake is predicted, a rational design can be achieved by providing the capacity to dissipate the imposed input energy [3, 4]. Input energy calculated for a single degree of freedom (SDOF) system can be used as a reliable estimate of the input energy for multi-story buildings [9]. Therefore, the first task in developing an energy based seismic design approach is the consistent prediction of input energy.

Input energy design spectra can be estimated from the basic strong motion intensity and hazard parameters which inherently depend on the source and site characteristics. Peak ground acceleration (PGA), peak ground velocity (PGV), PGV to PGA ratio (V/A ratio), effective duration, predominant period of ground motions, distance to fault, fault type, local soil condition and earthquake magnitude were identified as the distinctive parameters for determining the input energy spectra of earthquake ground motions in the past [5-10]. These studies were further extended to formulate input energy spectra in terms of ground motion intensity characteristics as well as structural system properties [12-28].

There are two basic approaches for defining input energy spectra in the current literature. In the first approach, design input energy is practically expressed in a piece-wise form bilinear or trilinear as an envelope spectrum for the earthquakes recorded in the corresponding seismic region [6, 9, 12-16, 21, 22]. Generally, the main purpose of these studies was to construct a demanding (enveloping) design spectra in the corresponding seismic regions. Design input energy spectra is obtained from attenuation relations [11, 19, 29], in the second approach. Attenuation relation approach was also used to predict absorbed energy for an inelastic system [17, 18]. Additionally, the relation between pseudo velocity (PS_V) spectrum and equivalent velocity (V_{eq}) spectrum were studied, and the ratio V_{eq}/PS_V was obtained for different earthquake magnitudes, source to site distances and soil types [19].

The initial step in energy based design at a broader context is the prediction of total input energy imposed by ground shaking, then estimating what portion of this energy is dissipated by hysteretic response, and finally checking whether the structural components have sufficient hysteretic energy dissipation capacity while maintaining the design performance objectives. This study focuses on the prediction of input energy as a first step in developing an energy based earthquake resistant design approach.

2. Strong Ground Motion Database

The influence of earthquake ground motion characteristics on input energy is investigated by employing a large number of strong ground motion (GM) records selected from the NGA database. The ground motion records in the data set, each one containing accelerograms of two horizontal components representing a free field motion, were selected from 104 earthquakes which occurred in different regions in the world. The selection criteria for the ground motions were that the moment magnitudes (M_w) are larger than 5, and peak ground acceleration values (PGA) of the records are larger than $0.05g$ where g is the acceleration of gravity. Thus, the generated data ($M_w \geq 5.5$ and $PGA \geq 0.05g$) is composed of 1,442 pairs of ground motion records or 2,884 horizontal components. Fig. 1 shows the scatter diagram of M_w versus R for the ground motions used in the database and the distribution of records in the database with V_{S30} (shear wave velocity of the upper 30 meters of soil profile). The limiting velocity value dividing soft and stiff soil classes in this study is 360 m/s. Ground motion sites in the database with V_{S30} values larger than the limiting value (NEHRP A, B and C) are designated as stiff soil type, and those with lower V_{S30} values than the limiting value (NEHRP D and E) are specified as soft soil type.

Soil class (S), distance to epicenter (R), moment magnitude (M_w) and fault mechanism type are selected as the basic parameters in order to characterize source and site properties in input energy computations. The fault directivity and pulse effects are not included in the prediction equation of input energy spectra.

3. Elastic Input Energy

Input energy demand on a linear elastic SDOF system can be obtained by integrating the equation of motion over displacement as shown in Eq. (1), where m , c and k are mass, viscous damping and stiffness of the SDOF system respectively, u is the relative displacement of the SDOF system with respect to the ground and \ddot{u}_g is the ground acceleration. Eq. (1) can be rearranged in Eq. (2), where E_K is the kinetic energy, E_S is the recoverable strain energy and E_D is the energy dissipated by viscous damping. The right hand side of Eq. (2) expresses the total input energy, as the work done by the equivalent seismic force - $m\ddot{u}_g(t)$ on the relative displacement of SDOF system relative to the ground.

$$\int_0^{u(t)} m \ddot{u}(t) du + \int_0^{u(t)} c \dot{u}(t) du + \int_0^{u(t)} k u du = - \int_0^{u(t)} m \ddot{u}_g(t) du \quad (1)$$

$$E_K(t) + E_D(t) + E_S(t) = E_I(t) \quad (2)$$

The total input energy E_I which is calculated at the end of ground motion duration is entirely dissipated by viscous damping in a linear elastic system. Elastic input energy can be converted into equivalent velocity (V_{eq}) in order to eliminate the dependence on mass by using Eq. (3).

$$V_{eq} = \sqrt{(2 E_I / m)} \quad (3)$$

In the foregoing analysis, the elastic input energy spectrum of each GM is obtained as equivalent velocity V_{eq} spectrum where V_{eq} is calculated as the geometric mean of the two horizontal components of each GM as shown in Eq. (4). Viscous damping ratio in Eq. (1) is taken as 5%.

$$V_{eq} = \sqrt{(V_{eq,H1}) * (V_{eq,H2})} \quad (4)$$

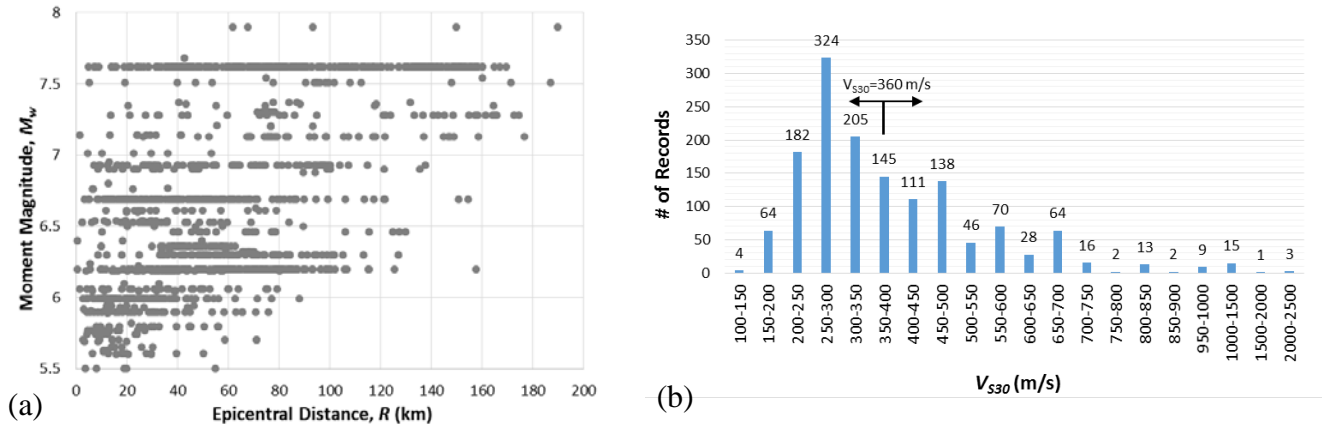


Fig. 1 – (a) Magnitude - distance distribution of ground motions used in this study (b) Distribution of ground motions in the database with V_{S30}

4. Prediction of Input Energy Spectrum

An energy based approach in seismic design requires an energy dissipation capacity for a structural system which is capable of dissipating the input energy demand while the system satisfies basic performance limit states. Therefore, it is required to describe the design input energy spectrum for the design site. Two approaches have been developed in this study for estimating input energy spectrum for a site. In the first approach, V_{eq} spectrum of a strong ground motion from an earthquake source is estimated by using the attenuation relation based on soil type, distance to fault, earthquake magnitude and fault mechanism. In the second approach, V_{eq} spectrum is obtained from its associated pseudo velocity (PS_V) spectrum by using a scaling operation between them. Therefore, the two approaches suggested below can be respectively classified as deterministic and probabilistic.

4.1 Input energy prediction by attenuation relations

Attenuation relations provide a description for an intensity parameter in terms of the basic source and site parameters. They are obtained by fitting a functional form to an empirical data through regression analyses. The attenuation relation developed by Akkar and Bommer [30-32] is employed in this study. Their attenuation function is given in Eq. (5) below.

$$\log(V_{eq}) = b_1 + b_2 M + b_3 M^2 + (b_4 + b_5 M) \log \sqrt{R_{jb}^2 + b_6^2} + b_7 S_S + b_8 S_A + b_9 F_N + b_{10} F_R \quad (5)$$

M is the moment magnitude here, R_{jb} is the Joyner-Boore distance in kilometers, S_S and S_A take binary values of 1 for soft and stiff soils and zero otherwise. F_N and F_R take values of 1 for normal and reverse ruptures, and 0 otherwise. The attenuation relation in Eq. (5) has been modified with respect to the seismic design practices and the parameters related to the earthquake characteristics and fault types associated with the GM records utilized in this study. For this purpose, epicentral distance R is used as the distance parameter instead of R_{jb} , and terms $b_7 S_S$ and $b_8 S_A$ related to the soil type are combined and labeled as $b_7 S$ in which S is equal to 1 for soft soil and 0 otherwise. When all these changes are implemented, Eq. (5) reduces to Eq. (6).

$$\log(V_{eq}) = b_1 + b_2M + b_3M^2 + (b_4 + b_5M)\log\sqrt{R^2 + b_6^2} + b_7S + b_8F_N + b_9F_R \quad (6)$$

The undetermined coefficients in Eq. (6) were determined by nonlinear regression analysis conducted at the specified period values. The regression coefficients in Eq. (6) and the corresponding standard deviations σ at each period are presented in Table 1. Furthermore, residuals between observed and estimated V_{eq} values were computed by using the expression given in Eq. (7). The best fit lines of these residuals relative to R and M were also obtained in order to reveal whether the estimated results from the attenuation relation are unbiased or biased with respect to the parameters R and M .

$$Res = \log(V_{eq_{est.}}) - \log(V_{eq_{obs.}}) \quad (7)$$

In order to evaluate the estimation accuracy of Eq. (6), the variation of 5% damped V_{eq} with distance R is obtained and plotted for selected earthquakes with two different moment magnitudes for the mean and mean \pm one standard deviation at three specified periods of 0.5 and 2.0 seconds. Then, the computed (observed) V_{eq} spectral values of the ground motions from the selected earthquakes at these specified periods were plotted on the related graphics in scatter form. Chi-Chi (1999) and Northridge-01 (1994) earthquakes with respective moment magnitudes of 7.62 and 6.69 were selected for comparative evaluation. Fault rapture mechanisms of these earthquakes were reverse-oblique and reverse, respectively. Fig. 2 and Fig. 3 present the comparisons of the computed V_{eq} spectral ordinates with the mean \pm sigma variations of V_{eq} obtained from the proposed attenuation relation (Eq. (6) and Table 1) for stiff and soft soil ground motions recorded during the selected earthquakes. It can be inferred from these figures that the observed V_{eq} spectral values generally fall within the range of mean \pm one standard deviation.

Mean V_{eq} spectra of ground motions selected from the Northridge-01 ($M_w=6.69$) and Chi-Chi ($M_w=7.62$) earthquakes are estimated by the attenuation relation developed in this study. The range of distances for the selected records are 17 - 23 km for the Northridge-01 (1994) and 48 - 51 km for the Chi-Chi (1999) earthquakes. The computed V_{eq} spectra of the selected ground motions from these two earthquakes are shown in Fig. 4 and Fig. 5 for stiff and soft soil types, along with their mean spectra and the estimated mean spectra from the proposed attenuation model. The middle values of the R bands of the records for each earthquake and each soil type are used for calculating the estimated mean spectra. It can be observed from Fig. 4 and Fig. 5 that the mean spectra estimated by the proposed attenuation model predicts the computed mean spectra with fairly good accuracy.

The sensitivity of V_{eq} spectra to magnitude, distance and fault type is assessed by utilizing the developed model for three magnitudes, three fault distances and three fault types, which are presented comparatively in Fig. 6, Fig.7 and Fig. 8. It can be observed from Fig. 6 - 8 that reverse and strike-slip faults impose 50 to 70% higher energy demands (V_{eq}^2) compared to normal faults. The effect of soil type is more prominent at larger magnitudes (M_w 6.5 and 7.5) where ground motions on soft soils are significantly more energy demanding than those on stiff sites. The soft-to-stiff V_{eq} ratio is about 1.5 for M_w 7.5 and 1.35 for M_w 6.5. Furthermore, energy demand from large earthquakes (M_w 7.5) do not fall off with period regardless of the fault distances. This is perhaps a crucial observation which reveals that energy based approaches are primarily worthwhile for longer period structures ($T > 1$ s) where seismicity is dominated by major faults which can produce large magnitude earthquakes. Moderate (M_w 6.5) to small magnitude (M_w 5.5) earthquakes impose highest energy demands on the short to medium period structures where $T < 1$ s.

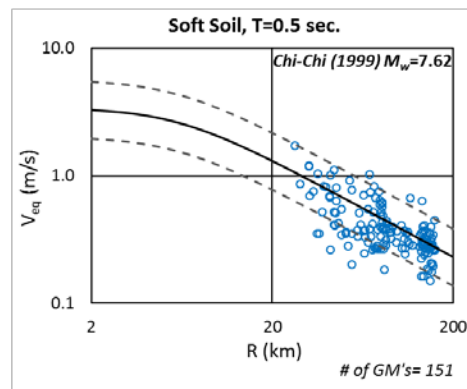
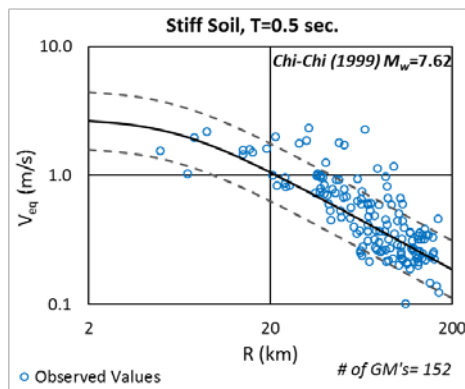
4.2 Input energy prediction by developing scaling relations between PS_V and V_{eq}

Housner [3] suggested in early 1950's that the velocity spectra can be considered as an intensity measure of the ground motion in terms of energy, where the amount of energy dissipated by the system is equal to the difference between the total input energy and the elastic strain energy. The correlation of elastic input energy spectrum, expressed in terms of V_{eq} , with the pseudo velocity spectrum PS_V is investigated herein. Magnitude, distance, soil type, period and damping ratio dependence of the V_{eq} / PS_V ratio is evaluated. For this purpose, V_{eq} / PS_V spectra for 5% damping are computed for the ground motions from Chi-Chi (1999) and Northridge-01 (1994) earthquakes, for stiff and soft sites separately. The V_{eq} / PS_V spectra computed for the ground motions

from two earthquakes are shown in Fig. 9. It can be observed from each box in Fig. 9 that the record-to-record variability of the V_{eq} / PS_V ratio for ground motions from the same earthquake on similar soil type, but from different distances are small. Moreover, mean spectra of ground motions in each box are quite similar for the two earthquakes and two soil types, which motivates the consideration of V_{eq} / PS_V spectrum as independent from magnitude, distance and soil type. This is somewhat expected since the effects of these parameters on V_{eq} and PS_V are quite similar.

Table 1 – Regression coefficients calculated for the attenuation model

T (sec.)	b ₁	b ₂	b ₃	b ₄	b ₅	b ₆	b ₇	b ₈	b ₉	σ
0.04	-6.7311	1.1311	-0.0292	1.4329	-0.3451	5.9923	-0.0132	-0.1766	-0.0675	0.286
0.10	-6.8986	1.5091	-0.0634	1.1510	-0.3019	7.9587	-0.0067	-0.1525	-0.0669	0.266
0.20	-7.8848	1.9630	-0.1034	0.6448	-0.2131	7.4717	0.0278	-0.0506	-0.0332	0.213
0.30	-7.2983	1.7988	-0.0929	0.4769	-0.1745	4.8839	0.0581	-0.0697	0.0055	0.205
0.40	-7.9272	1.9987	-0.1082	0.3038	-0.1461	5.5817	0.0757	-0.0336	0.0225	0.211
0.50	-6.7183	1.6872	-0.0885	0.0349	-0.1050	5.9564	0.0916	-0.0407	0.0339	0.223
0.60	-7.7329	2.0915	-0.1268	-0.5247	-0.0178	5.1838	0.1025	-0.0523	0.0397	0.233
0.70	-8.0485	2.2630	-0.1451	-0.9481	0.0435	4.8084	0.1136	-0.0664	0.0491	0.244
0.80	-7.2850	1.9890	-0.1217	-0.8404	0.0276	5.1292	0.1281	-0.0638	0.0472	0.250
0.90	-7.9541	2.1704	-0.1342	-0.8630	0.0329	5.4492	0.1319	-0.0656	0.0468	0.256
1.00	-8.2500	2.2375	-0.1387	-0.8459	0.0338	5.7942	0.1400	-0.0633	0.0500	0.264
1.20	-8.9064	2.3680	-0.1447	-0.6941	0.0151	5.0968	0.1622	-0.0892	0.0279	0.281
1.40	-9.4288	2.4217	-0.1417	-0.4186	-0.0252	5.1836	0.1762	-0.0987	0.0132	0.289
1.50	-9.9234	2.5239	-0.1462	-0.3064	-0.0420	4.8461	0.1801	-0.1098	0.0135	0.292
1.60	-10.4924	2.6607	-0.1542	-0.2487	-0.0507	4.7773	0.1837	-0.1052	0.0102	0.295
1.80	-10.6677	2.6649	-0.1526	-0.2112	-0.0527	4.3636	0.1980	-0.0924	0.0052	0.302
2.00	-10.6616	2.6143	-0.1461	-0.1138	-0.0662	4.1496	0.1986	-0.0848	0.0046	0.311
2.50	-11.2925	2.7023	-0.1453	0.1255	-0.1057	5.4719	0.1993	-0.1232	0.0059	0.328
3.00	-10.8501	2.4319	-0.1162	0.4613	-0.1543	5.9322	0.2003	-0.1206	-0.0136	0.335
3.50	-9.7835	2.0297	-0.0798	0.5842	-0.1773	7.7649	0.1984	-0.1204	-0.0304	0.332
4.00	-9.1531	1.8696	-0.0699	0.3064	-0.1395	8.8112	0.1958	-0.1442	-0.0476	0.328



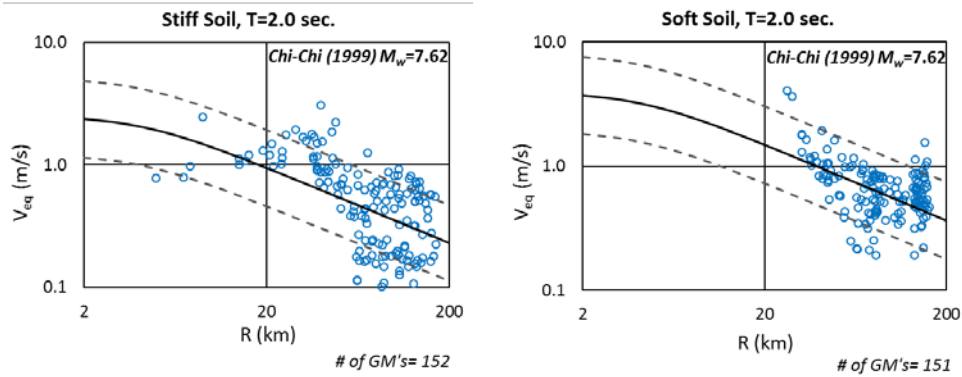


Fig. 2 – Comparison of the computed V_{eq} with the mean and mean \pm one standard deviations of the attenuation model for $M_w=7.62$ Chi-Chi (1999) earthquake, for stiff and soft soil types.

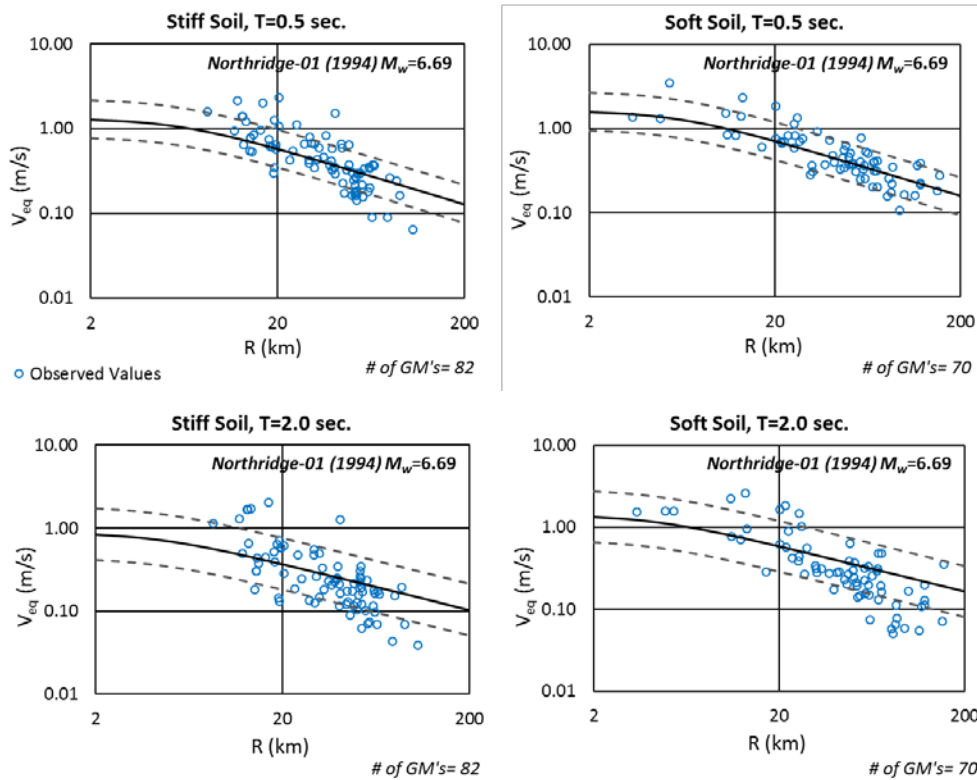


Fig. 3 – Comparison of the computed V_{eq} with the mean and mean \pm one standard deviations of the attenuation model for $M_w=6.69$ Northridge-01 (1994) earthquake, for stiff and soft soil types.

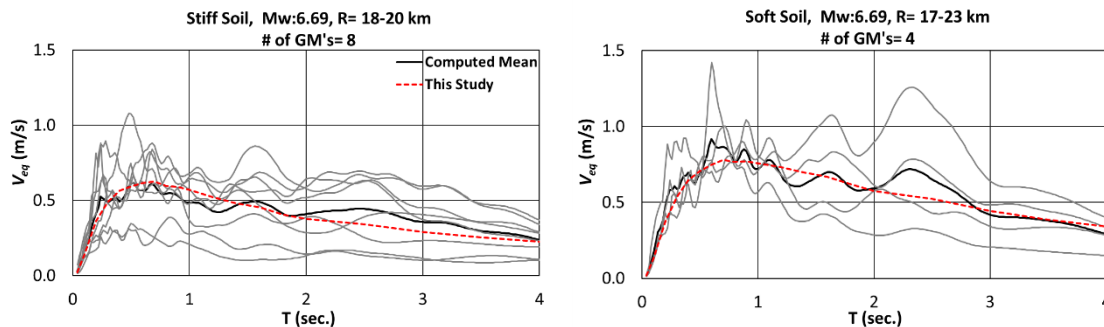


Fig. 4 – V_{eq} spectra of ground motions selected from Northridge-01 (1994) earthquake and the comparison of their mean spectra with the estimated mean from Eq. (6).

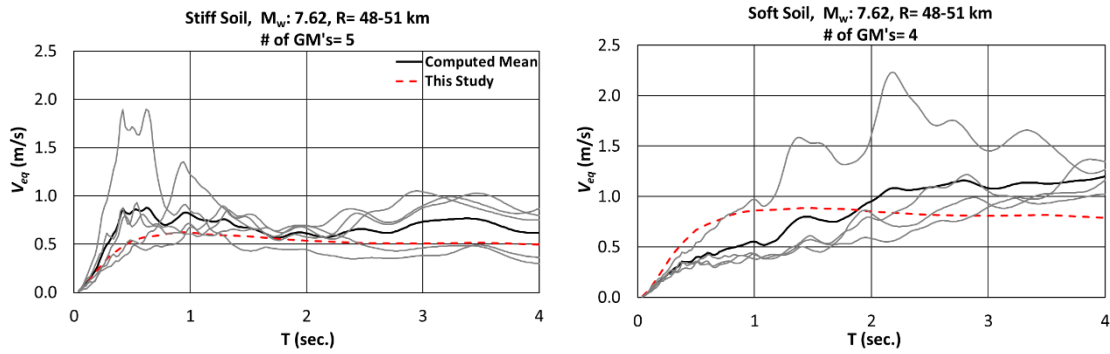


Fig. 5 – V_{eq} spectra of ground motions selected from Chi-Chi (1999) earthquake and the comparison of their mean spectra with the estimated mean from Eq. (6).

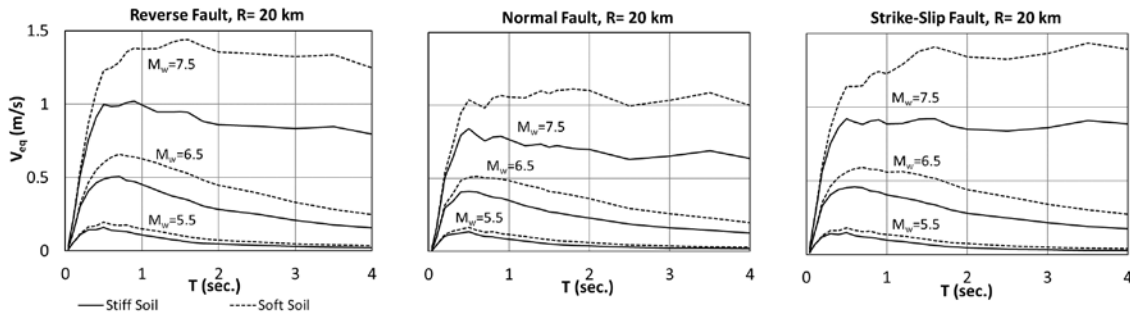


Fig. 6 – Variation of input energy spectra V_{eq} with earthquake magnitude obtained from the attenuation model for different soil types and fault mechanisms at $R=20$ km.

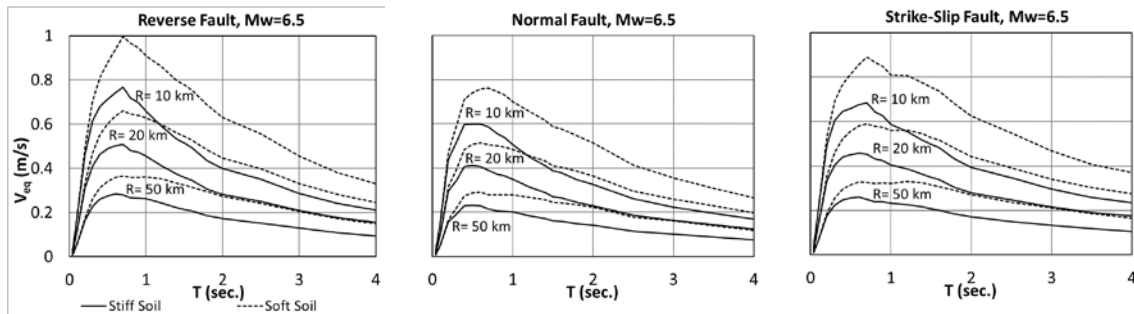


Fig. 7 – Variation of input energy spectra V_{eq} with epicentral distance obtained from the attenuation model for different soil types and fault mechanisms, $M_w=6.5$.

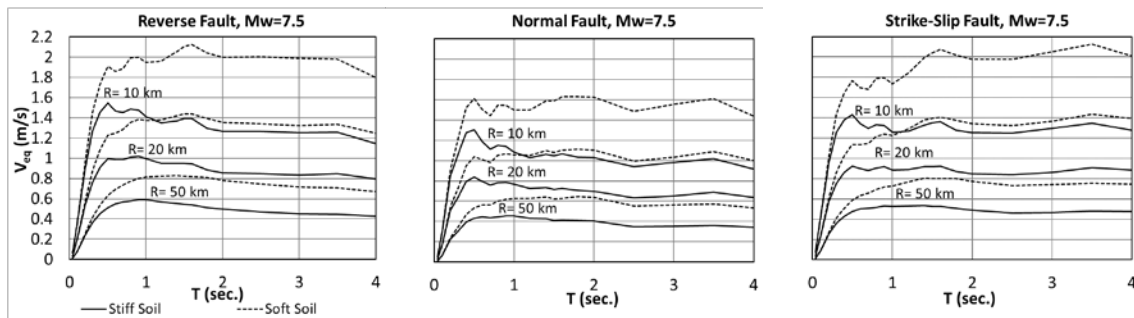


Fig. 8 – Variation of input energy spectra V_{eq} with epicentral distance obtained from the attenuation model for different soil types and fault mechanisms, $M_w=7.5$.

For further investigation of the sensitivity of V_{eq} / PS_V spectrum to magnitude and soil type, mean spectral curves of the ground motions from five earthquakes (Chi-Chi (1999) - M_w 7.62, Hector Mine (1999) - M_w 7.13, Loma Prieta (1989) - M_w 6.93, Northridge-01 (1994) - M_w 6.69 and Whittier Narrows-01 (1987) - M_w 5.99) and

each soil type are compared in Fig. 10. There is no consistently noticeable effect of magnitude and soil type on V_{eq} / PS_V spectra in Fig. 10. Past studies have showed that V_{eq} / PS_V is mainly influenced by the fraction of inherent damping of the structure [19]. In order evaluate the dependence on damping, the mean V_{eq} / PS_V spectra for 2% and 10% damping ratios of ground motions in the database are computed and compared with the 5% damped spectra in Fig. 11. As it was expected that with increased damping PS_V values decreases, and the obtained V_{eq} / PS_V ratios increases as in Fig. 11, since spectral input energy values does not vary much with the damping ratio, but get smoother for higher damping ratios [27]. Hence, V_{eq} / PS_V spectrum can be idealized by a simple function of T only for a selected damping value. The exponential model in Eq. (8) is used for expressing this idealization where the coefficients a , b and c are all functions of vibration period. The undetermined coefficients in Eq. (8) were obtained by regression analysis, by employing V_{eq} and PS_V spectra of ground motions in the database for 2%, 5% and 10% damping ratios, separately. They are presented in Table 2.

$$V_{eq}/PS_V = a \cdot e^{-bT} + c \quad (8)$$

Once the V_{eq} / PS_V spectrum is estimated from Eq. (8) and Table 2 for the selected damping ratio, input energy demand on a SDOF system can be calculated by scaling the corresponding PS_V spectra with the spectral V_{eq} / PS_V ratio. The mean V_{eq} / PS_V spectrum estimated from Eq. (8) and Table 2 for 5% damping is compared with the mean computed V_{eq} / PS_V spectrum of all ground motions in the database in Fig.12(a). Mean \pm sigma variation of the computed V_{eq} / PS_V spectra are also presented in Fig. 12(a). In addition, the mean V_{eq} / PS_V spectra estimated for three damping ratios are presented in Fig. 12(b). It is observed that the estimated and the computed mean spectra match almost exactly.

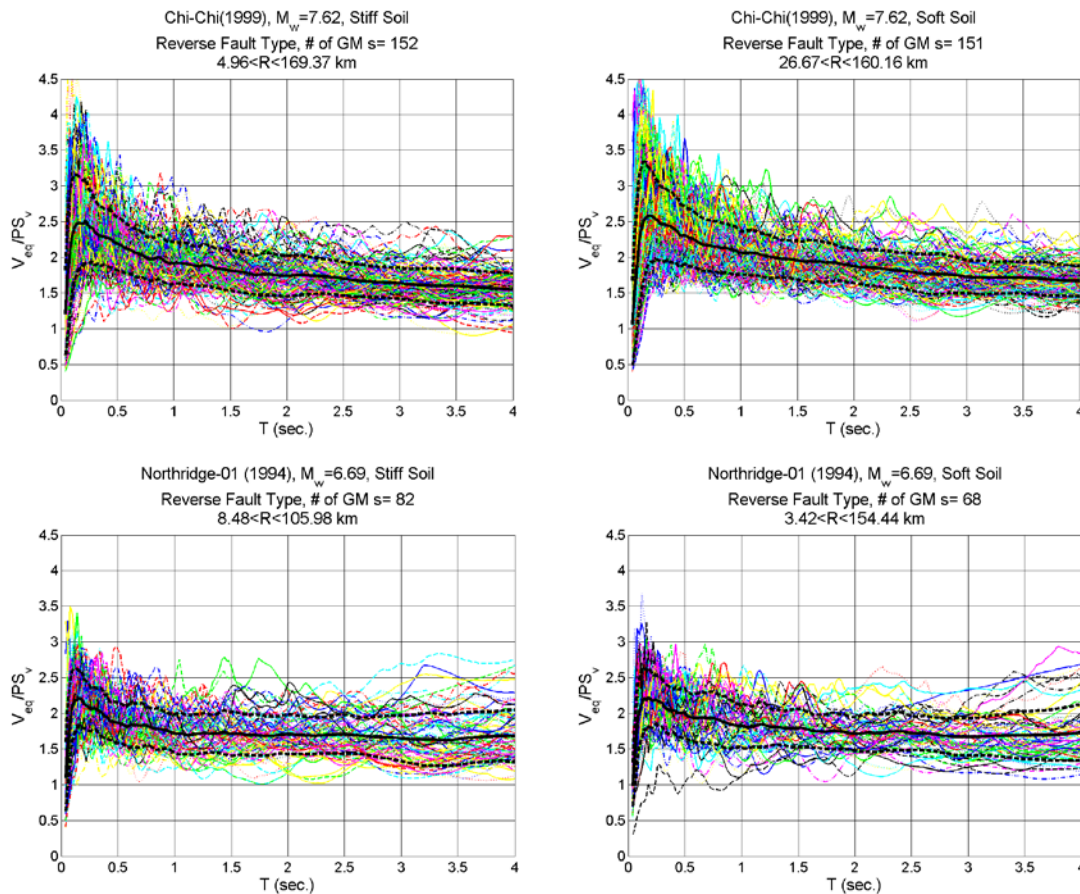


Fig. 9 – Spectral variations of 5 percent damped V_{eq} / PS_V ratio for GM's from Chi-Chi (1999) and Northridge-01 (1994) earthquakes on stiff and soft sites, along with their mean (solid) and mean \pm sigma (dashed) spectra.

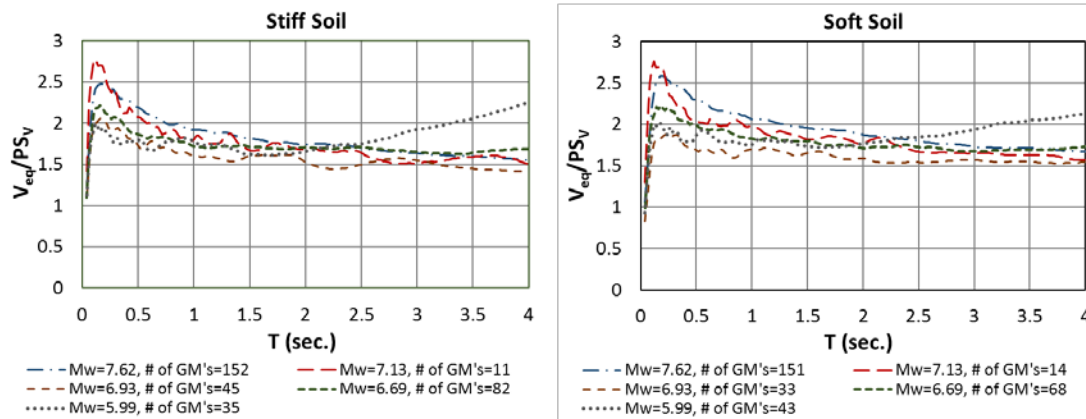


Fig. 10 – Comparison of the mean 5 percent damped V_{eq} / PS_V ratios of ground motions from the selected earthquakes for stiff and soft soil types.

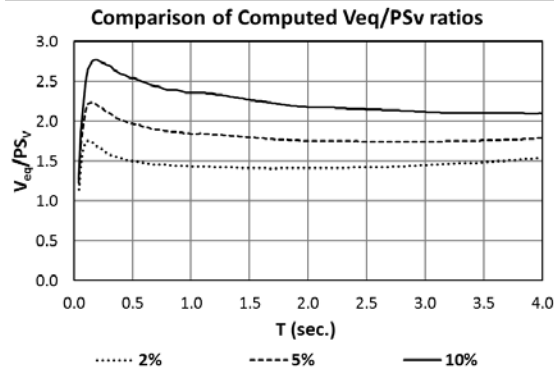


Fig. 11 – Comparison of the mean 5 percent damped V_{eq} / PS_V spectra with the mean 2 and 10 percent damped spectra for the ground motions in the database

Table 2 – Coefficients for the model equation of V_{eq}/PS_V versus T for different damping ratios

T (sec.)	2% Damping			5% Damping			10% Damping		
	a	b	c	a	b	c	a	b	c
0.04	0.6662	9.8456	0.6913	0.7066	8.6722	0.7266	0.7321	7.9524	0.7493
0.1	0.9367	1.6342	0.9429	1.0832	0.1650	1.0750	1.1973	-1.0100	1.1740
0.2	0.9433	1.2842	0.9536	1.1458	0.2638	1.1178	1.3265	-0.7183	1.2435
0.3	0.9300	1.2340	0.9483	1.1501	0.4944	1.1097	1.3555	-0.2593	1.2340
0.4	0.9325	1.1691	0.9549	1.1598	0.5955	1.1055	1.3752	-0.0035	1.2190
0.5	0.9402	1.1199	0.9638	1.1831	0.6280	1.1087	1.4110	0.1088	1.2077
0.6	0.9573	1.0712	0.9766	1.2082	0.6457	1.1110	1.4459	0.1828	1.1932
0.7	0.9710	1.0415	0.9856	1.2369	0.6524	1.1130	1.4837	0.2275	1.1759
0.8	1.0037	0.9954	1.0016	1.2730	0.6464	1.1158	1.5229	0.2559	1.1551
0.9	1.0296	0.9671	1.0120	1.3155	0.6323	1.1178	1.5766	0.2511	1.1257
1.0	1.0552	0.9447	1.0203	1.3565	0.6211	1.1164	1.6276	0.2466	1.0891
1.1	1.0924	0.9157	1.0306	1.4106	0.5953	1.1140	1.6896	0.2214	1.0344
1.2	1.1313	0.8897	1.0391	1.4566	0.5797	1.1065	1.7446	0.2203	1.0020
1.3	1.1674	0.8695	1.0448	1.5068	0.5595	1.0955	1.7956	0.3269	1.1461
1.4	1.2090	0.8475	1.0500	1.5570	0.5395	1.0804	1.8470	0.3170	1.1108
1.5	1.2509	0.8276	1.0534	1.6061	0.5204	1.0613	1.8981	0.3048	1.0685
1.6	1.3005	0.8039	1.0563	1.6614	0.4945	1.0354	1.9527	0.2860	1.0146
1.7	1.3420	0.7872	1.0562	1.7156	0.4697	1.0040	2.0076	0.2650	0.9492
1.8	1.4065	0.7556	1.0563	1.7741	0.4506	0.9811	2.1992	0.4910	1.2982
1.9	1.4579	0.7336	1.0529	1.8255	0.5150	1.0735	2.2743	0.4911	1.2947
2.0	1.5162	0.7071	1.0470	1.8840	0.4908	1.0477	2.3548	0.4890	1.2922

2.2	1.6390	0.6491	1.0246	2.0144	0.4259	0.9634	2.5288	0.4784	1.2888
2.4	1.7752	0.5871	0.9892	2.3087	0.5874	1.1859	2.6919	0.4666	1.2793
2.6	1.9016	0.5966	1.0219	2.4826	0.5719	1.1844	2.8431	0.4501	1.2640
2.8	2.1786	0.6777	1.1070	2.6554	0.5541	1.1805	2.9707	0.4280	1.2383
3.0	2.3907	0.6510	1.1119	2.8201	0.5319	1.1734	3.0649	0.3998	1.1945
3.5	2.8736	0.5813	1.1102	3.1056	0.4451	1.1053	3.1822	0.2616	0.8325
4.0	3.1446	0.4549	1.0317	4.6007	0.5093	1.1877	5.2470	0.4583	1.2609

Probabilistic seismic hazard maps and the associated seismic design guidelines provide linear elastic acceleration design spectra for a geographical location, for several return periods or probabilities of exceeding a given spectral acceleration intensity parameter, which leads to uniform hazard spectrum. Converting a design acceleration spectrum to pseudo velocity spectrum for a given damping ratio is a standard practice. Then the input energy spectrum in the probabilistic hazard family can be obtained by applying the spectral scaling ratio V_{eq} / PS_V derived above, to the PS_V spectrum.

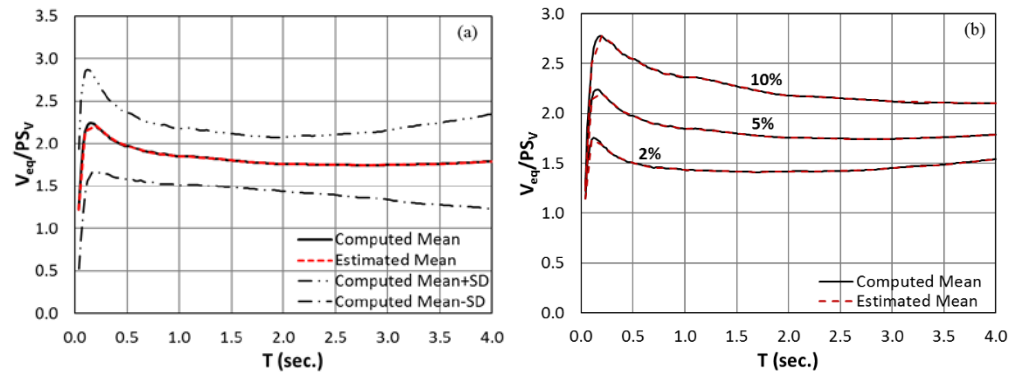


Fig. 12 – (a) Comparison of the estimated mean with the computed mean, and mean \pm sigma V_{eq} / PS_V spectra of all ground motions in the database for 5 percent damping. (b) Comparison of the estimated and computed mean V_{eq} / PS_V spectra for 2, 5 and 10 percent damping

A high seismic intensity location was selected in the United States, and the 5 percent damped acceleration design spectra based on NEHRP [33] provisions (2/3 of the 2475-year spectrum) were obtained for stiff (C) and soft (D) soil types, as shown in Fig. 13. Then ground motions were selected from the NGA database where 0.2 and 1 second period spectral accelerations were sufficiently close to the NEHRP design spectra for stiff and soft soil types. Fig. (13) shows the NEHRP design spectra and the acceleration spectra of the selected earthquake ground motions along with their mean spectra for each soil type separately. After calculating PS_V spectra from the associated NEHRP 5 percent damped acceleration design spectra given in Fig. 13 for each soil type, V_{eq} values were obtained by using Eq. (8) and the coefficients for 5 percent damping given in Table 2. The comparison of the V_{eq} design spectra obtained by scaling the NEHRP design spectra and the mean V_{eq} spectra of the selected (spectrum compatible) GM records are shown in Fig. 14. It can be observed that the design V_{eq} spectra based on NEHRP provisions exhibit a good agreement with the mean spectra of the selected GM records along the entire period range.

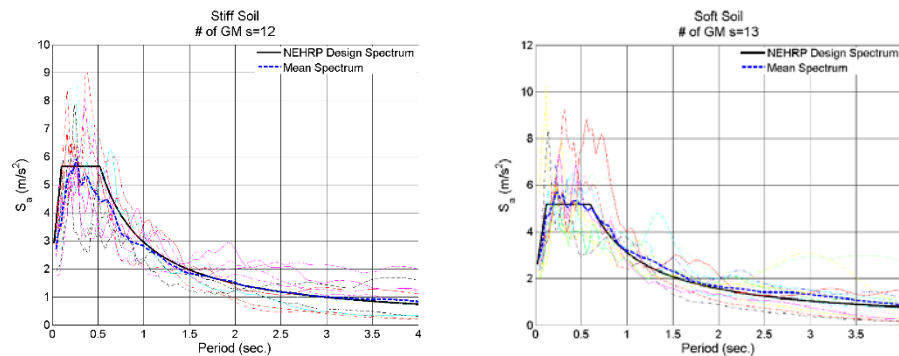


Fig. 13 – 5 percent damped design acceleration spectra based on NEHRP provisions, and acceleration spectra of the selected ground motions along with their mean spectrum

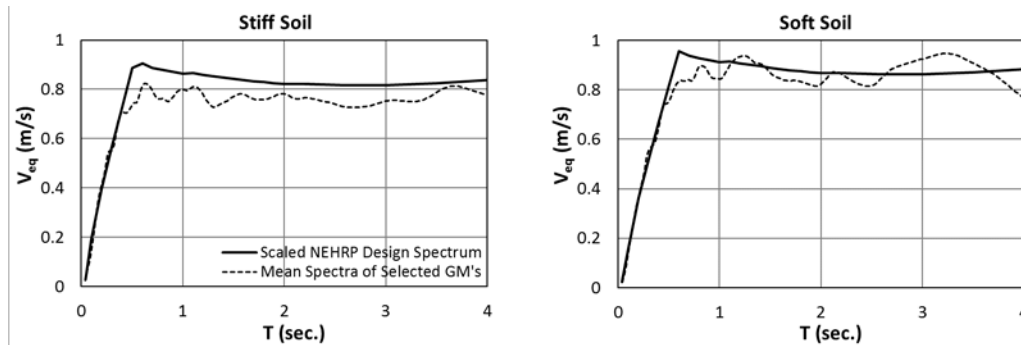


Fig. 14 – Scaled V_{eq} spectra based on NEHRP design acceleration spectra, and its comparison with the mean spectra of the selected (spectrum compatible) ground motions

5. Conclusion

The purpose of this study is to develop simple but reliable models for predicting input energy spectra. Two approaches have been employed. An attenuation model has been developed through nonlinear regression analysis in the first approach. Comparative results obtained by this model revealed that earthquakes which occur on reverse and strike slip faults impose larger energy demands than the earthquakes on normal faults. The effect of soil type on input energy is more significant for larger magnitude earthquakes where ground motions on soft soil sites impose significantly larger energy demands compared to those on stiff sites. Input energy is generally largest at the short to medium period ranges under the ground motions from small to moderate magnitude earthquakes whereas this period range includes long period structures under the ground motions from large magnitude earthquakes.

The second approach utilizes probabilistic seismic hazard maps. Input energy spectrum at a site can be directly obtained from the associated acceleration design spectrum by applying simple scaling relations developed in this study. Reliability of input energy spectra predicted by both approaches have been tested and verified through comparisons with the input energy imposed by ground motions recorded on different soil sites during different magnitude earthquakes. Input energy imposed on structures during strong earthquakes can be confidently obtained by using the models proposed in this study. Input energy is crucial for estimating the duration dependent cyclic degradation effects in structures for a realistic seismic performance evaluation.

6. References

- [1] Erberik MA, Sucuoğlu H (2004): Seismic energy dissipation in deteriorating systems through low-cycle fatigue. *Earthquake Engineering and Structural Dynamics*, **33** (1), 49-67.
- [2] Acun B, Sucuoğlu H (2010): Performance of reinforced concrete columns designed for flexure under severe displacement cycles. *ACI Structural Journal*, **107** (3), 364-371.
- [3] Housner GW (1956): Limit design of structures to resist earthquakes. *In Proceedings of the World Conference on Earthquake Engineering*, Berkeley, California.
- [4] Housner GW (1959): Behavior of Structures during Earthquake. *Journal of Engineering Mechanics Divisions*, **85**, 109-129.
- [5] Sucuoğlu H, Nurtuğ A (1995): Earthquake ground motion characteristics and seismic energy dissipation. *Earthquake Engineering and Structural Dynamics*, **24**, 1195-1213.
- [6] Fajfar P, Vidic T, Fischinger M (1989): Seismic demand in medium- and long-period structures. *Earthquake Engineering and Structural Dynamics*, **18**, 1133-1144.
- [7] Uang CM, Bertero VV (1988): Implications of recorded earthquake ground motions on seismic design of building structures. *Technical Report PEER 88/13*, Pacific Earthquake Engineering Research, Berkeley, USA.

- [8] Zahran TF, Hall WJ (1984): Earthquake energy absorption in sdof structures. *Journal of Structural Engineering*, **110** (8), 1757-1772.
- [9] Akiyama H (1988): Earthquake resistant design based on the energy concept. *In Proceeding of 9th World Conference on Earthquake Engineering*, Tokyo and Kyoto, **V**, 905-910.
- [10] Uang CM, Bertero VV (1990): Evaluation of seismic energy in structures. *Earthquake Engineering and Structural Dynamics*, **19**, 77-90.
- [11] Ordaz M, Huerta B, Reinoso E (2003): Exact computation of input-energy spectra from Fourier amplitude spectra. *Earthquake Engineering and Structural Dynamics*, **32**, 597-602.
- [12] Benavent-Climent A, Pujades LG, Lopez-Almansa F (2002): Design energy input spectra for moderate seismicity regions. *Earthquake Engineering and Structural Dynamics*, **31**, 1151-1172.
- [13] Benavent-Climent A, Lopez-Almansa F, Bravo-Gonzales DA (2010) Design energy input spectra for moderate-to-high seismicity regions based on Colombian earthquakes. *Soil Dynamics and Earthquake Engineering*, **30**, 1129-1148.
- [14] Okur A, Erberik MA (2012): Adaptation of energy principles in seismic design of Turkish RC frame structures. Part I: Input Energy Spectrum. *In Proceedings of 15th World Conference on Earthquake Engineering*, Lisbon, Portugal.
- [15] Decanini LD, Mollaioli F (1998): Formulation of elastic earthquake input energy spectra. *Earthquake Engineering and Structural Dynamics*, **27**, 1503-1522.
- [16] Amiri GG, Darzi GA, Amiri JV (2008): Design elastic input energy spectra based on Iranian earthquakes. *Canadian Journal of Civil Engineering*, **35**, 635-346.
- [17] Chou CC, Uang CM (2000): Establishing absorbed energy spectra – an attenuation approach. *Earthquake Engineering and Structural Dynamics*, **29**, 1441-1455.
- [18] Chou CC, Uang CM (2003): A procedure for evaluating seismic energy demand of framed structures. *Earthquake Engineering and Structural Dynamics*, **32**, 229-244.
- [19] Chapman MC (1999): On the use of elastic input energy for seismic hazard analysis. *Earthquake Spectra*, **15**(4), 607-635.
- [20] McKevitt WE, Anderson DL, Cherry S (1960): Hysteretic energy spectra in seismic design. *Proceedings of 2nd World Conference on Earthquake Engineering*, Tokyo and Kyoto, **7**, 487-494.
- [21] Decanini LD, Mollaioli F (2001). An energy-based methodology for the assessment of seismic demand. *Soil Dynamics and Earthquake Engineering*, **21** (2), 113-137.
- [22] Fajfar P, Fischinger M (1990): A seismic design procedure including energy concept. *In Proceedings of the 9th European Conference on Earthquake Engineering*, Moscow, Russia, 312-321.
- [23] Fajfar P, Vidic T, Fischinger M (1992): On energy demand and supply in SDOF systems. *Nonlinear Seismic Analysis of Reinforced Concrete Buildings*, London, Elsevier, 48-71.
- [24] Fajfar P, Vidic T (1994): Consistent inelastic design spectra: strength and displacement. *Earthquake Engineering and Structural Dynamics*, **23**, 507-521.
- [25] Fajfar P, Vidic T (1994): Consistent inelastic design spectra: hysteretic and input energy. *Earthquake Engineering and Structural Dynamics*, **23**, 523-537.
- [26] Bruneau M, Wang N (1996): Normalized energy-based methods to predict the seismic ductile response of SDOF structures. *Engineering Structures*, **18** (1), 13-28.
- [27] Nurtuğ A, Sucuoğlu H (1995): Prediction of seismic energy dissipation in SDOF systems. *Earthquake Engineering and Structural Dynamics*, **24**, 1215-1223.
- [28] Manfredi G (2001): Evaluation of seismic energy demand. *Earthquake Engineering and Structural Dynamics*, **30**, 485-499.
- [29] Cheng Y, Lucchini A, Mollaioli F (2014): Proposal of new ground-motion prediction equations for elastic input energy spectra. *Earthquakes and Structures*, **7** (4), 485-510.
- [30] Akkar S, Bommer J (2007): Empirical prediction equations for peak ground velocity derived from strong-motion records from europe and middle east. *Bulletin of Seismological Society of America*, **97** (2), 511-530.



- [31] Akkar S, Bommer J (2007): Prediction of elastic displacement response spectra in Europe and the Middle East. *Earthquake Engineering and Structural Dynamics*, **36**, 1275-1301.
- [32] Akkar S, Bommer J (2010): Empirical equations for the prediction of PGA, PGV and spectral accelerations in Europe the Mediterranean Region, and the Middle East. *Seismological Research Letters*, **81** (2), 195-206.
- [33] NERHP (2015): *Recommended Seismic Provisions for New Buildings and Other Structures (FEMA P-1050-1/2015)*. Building Seismic Safety Council., Washington DC.